**Engineering and Technology Journal e-ISSN: 2456-3358**

**Volume 09 Issue 09 September-2024, Page No.- 5027-5039**

**DOI: 10.47191/etj/v9i09.07, I.F. – 8.227**



# Numerical Investigation of the Effects of Air Flow Geometry and Reynolds Number in Cooling Systems of Lithium-Ion Batteries

**Haydar Kepekci[1], Mehmet Emin Agca[2]**

[1]Mechatronics Engineering Department, Engineering-Architecture Faculty, Istanbul Gelisim University, Turkey

[2]Mechanical Engineering Department, Engineering-Architecture Faculty, Istanbul University-Cerrahpasa, Turkey

**ABSTRACT:** In this study, two factors affecting the cooling performance of lithium-ion batteries have been selected and investigated using numerical methods. They have been determined as airflow geometry design and different Reynolds numbers. First, the differences between a classical flow path design (Z channel) with air inlets and outlets in the same direction and an alternative design (U channel) with air inlets and outlets in different directions have been evaluated. To understand the effect of the turbulent properties of the fluid in both designs, the results of the analyses performed using different Reynolds numbers (Re=4000, 6000, 8000, 10000, 15000) have been compared with each other. As a result, it has been observed that the U-channel design provided more homogeneous cooling on the battery surfaces and that the heat transfer is at higher values. In addition, it was observed that the Nusselt number increased with the increase in the Reynolds numbers used in the analyses. This study provides important data to understand the effects of airflow geometry and Reynolds number on the design of lithium-ion battery cooling systems and contributes to the development of optimized cooling solutions.

**KEYWORDS:** Lithium-Ion battery cooling, airflow geometry, Reynolds number, turbulent flow

## 1. INTRODUCTİON

Lithium-ion batteries have become one of the important components of developing technology. These batteries are widely used especially in portable electronic devices, electric vehicles and renewable energy storage systems. Thanks to their high energy density, lithium-ion batteries, which can store large amounts of energy despite their small size, are frequently used in smartphones, laptops and tablets, which are indispensable parts of daily life. In addition, with the increasing prevalence of environmentally friendly electric cars instead of fossil fuels, the energy efficiency and long life of these batteries have revolutionized the transportation sector [1]. Many advantages of lithium-ion batteries support their widespread use. First, their high energy density allows for longer life than other types of batteries. Their lightweight construction offers a major advantage in applications where weight is important, such as portable devices and electric vehicles [2]. In addition, the low self-discharge rate allows lithium-ion batteries to be stored for long periods without being charged. Their long life is also one of the reasons why these batteries are preferred. Durability in charge-discharge cycles provides cost-effectiveness and reduces environmental impacts. These advantages are the main reasons why lithium-ion batteries are preferred [3].

The advantages offered by lithium-ion batteries are not limited to portability and energy density. These batteries, which also offer significant environmental benefits, stand out as an environmentally friendly alternative because they contain less toxic substances and are recyclable. Compared to older battery types such as lead-acid or nickel-cadmium, the production and usage processes of lithium-ion batteries are less harmful to the environment, making them an attractive option for industries seeking sustainable energy solutions. At the same time, the low maintenance requirements of these batteries provide an economic advantage for users by reducing additional costs during their lifespan [4]. Another promising area of use for lithium-ion batteries is their role in the integration of renewable energy sources. The intermittency of energy obtained from natural sources such as solar and wind necessitates storage solutions to ensure continuous energy supply. Lithium-ion batteries offer an ideal solution for storing this energy and using it when needed. In this context, the use of lithium-ion batteries is of critical importance to increase the efficiency of renewable energy systems and reduce dependence on fossil fuels [5].

As a result, lithium-ion batteries are a versatile and effective technology that offers a powerful answer to the need for energy storage and portability in the modern world. Used in a wide range of applications from electronic devices to electric vehicles, from medical applications to renewable energy systems, these batteries play an important role in every field of technology thanks to their high energy density, long life, environmentally friendly features and low maintenance requirements [6]. The development and proliferation of lithium-ion batteries will continue to shape both individual daily lives and global energy strategies. In the future, the role of lithium-ion batteries in energy storage and portable technology solutions will become increasingly central [7].

Lithium-ion batteries operate most efficiently within a specific temperature range. Typically, these batteries have an ideal operating temperature range of 20°C to 60°C [8]. In this temperature range, the battery's chemical reactions occur stably, achieving optimum performance in terms of both capacity and life. However, at low temperatures, battery performance drops significantly, which can lead to reduced energy density and longer charging times. At high temperatures, chemical reactions inside the battery accelerate, which can lead to thermal instability and compromise battery safety. Therefore, temperature management of lithium-ion batteries is critical for both safety and performance [9].

One of the biggest problems with lithium-ion batteries is the cooling difficulties encountered at high temperatures. Especially in high-energy applications such as electric vehicles, overheating of batteries poses a serious risk. Overheating can shorten the life of the battery and can also lead to a dangerous situation called thermal runaway. Thermal runaway means that the internal temperature of the battery increases uncontrollably, potentially causing a fire. To prevent this situation, lithium-ion batteries usually use cooling systems or materials that provide heat dissipation. However, these solutions create additional challenges in terms of both cost and system complexity. Therefore, it is important to develop an effective thermal management strategy to ensure the safe and efficient operation of lithium-ion batteries.

There are many studies on this subject in the literature. Şen et al. reviewed the working principle, performance and failures of lithium-ion batteries. In their study, they focused on the general problems of batteries used in electric vehicles [10]. Deng et al. reviewed the research on the performance of coolant for lithium-ion batteries and the classification of liquid cooling systems. They compared the applications of different liquids such as water and oil as coolants and different additives such as nanoparticles. They evaluated the differences between active and passive cooling, internal and external cooling, and direct and indirect cooling for the classification of liquid cooling systems [11]. Chen et al. compared four cooling methods for lithium-ion batteries. They were air cooling, direct liquid cooling, indirect liquid cooling, and fin cooling. They found that the air cooling system consumed about three times more energy than the other methods and the indirect liquid cooling system had the lowest maximum temperature increase [9]. Thakura et al. focused on the thermal management systems of lithium-ion batteries of electric vehicles and examined different cooling technologies. They found that air-cooled systems, although offering a simple and safe design, have a limited area of use due to their low heat capacity. They stated that while liquid-cooled systems provide more effective cooling, attention should be paid to the risk of leakage in their designs [12].

Sun and Dixon aimed to develop a cooling strategy for logistic ion air-cooled batteries used in hybrid vehicles. In the study, they created a three-dimensional thermal model for the temperature conditions and cooling distribution of the battery. As a result, a cooling strategy was developed to maximize the amount of battery pack and driving range [13]. Xun et al. investigated the differences between flat-plate and cylindrical designs to examine the thermal management of lithium-ion batteries. They found that in the flat-plate design, increasing the cooling channel size increased energy efficiency but caused irregularities in temperature distribution. They found that cylindrical battery designs were more efficient in terms of cooling, although less compact. They also added that a reverse flow arrangement or periodically changing the flow direction could improve thermal management [14]. Saw et al. focused on the air cooling system of a lithium-ion battery consisting of 38,120 cells for electric vehicles. The thermal performance of the battery was evaluated by computational fluid dynamics (CFD) method and experimental tests. They compared the results obtained from the analyses they made with different air flow rates with the data in the literature. As a result, they demonstrated the accuracy of the CFD method. They showed that the CFD method can be used to predict the thermal performance of large batteries [15]. Shang et al. designed a liquid cooling system for lithium-ion batteries and evaluated the cooling performance. They found that increasing the mass flow rate could not significantly improve the temperature distribution, although it reduced the maximum temperature [16]. Chavan et al. focused on extending the battery life by analyzing different cooling methods to ensure that lithium-ion batteries operate at optimum temperatures in electric vehicles. In their study, they presented different design suggestions for this issue [17]. Wang et al. investigated forced air cooling methods for thermal management of lithium-ion batteries. They evaluated the thermal behaviour of batteries under different cooling conditions and ambient temperatures using three-dimensional computational fluid dynamics (CFD). As a result, they found that forced air cooling is necessary above 35°C [18].

Park has studied and modelled the cooling of lithium-ion batteries used in hybrid electric vehicles with a forced air cooling system. In his study, he showed that battery cooling performance can be optimized by evenly distributing the air flow [19]. Akbarzadeh et al. compared air and liquid cooling systems for lithium-ion batteries and studied their power consumption and cooling performance. As a result, they found that liquid systems provide lower module temperature and better temperature distribution for a given power consumption [8]. Yang et al. investigated the thermal performance of axial flow air cooling for lithium-ion batteries. They evaluated the effects of radial spacing and airflow between cells by numerical analysis. As a result, they found that wider radial spacing makes the temperature distribution more uniform, slightly increases the average temperature, and reduces the energy cost of the cooling system [20]. Kizilel et al. evaluated the passive thermal management system for Li-ion batteries using phase change material (PCM). They found that passive cooling provides faster heat dissipation than active cooling [21]. Wang et al. investigated the thermal performance of different cell arrangements of lithium-ion batteries. By evaluating air cooling strategies with various cell arrangements and fan positions, they found that the best cooling performance was achieved when the fan was placed on top of the module. They also determined that the cubic arrangement was the most cost-effective structure [22]. Kirad and Chaudhari studied the effectiveness of a forced air cooling system for lithium-ion batteries. They developed numerical models for a module consisting of 30 lithium-ion batteries and validated them with literature data. They found that changes in longitudinal and transverse distance between batteries greatly impact cooling efficiency and temperature distribution [23]. Wang et al. investigated the liquid cooling systems used in the thermal management of lithium-ion batteries for electric vehicles and proposed an innovative modular liquid cooling system. They examined the effects of coolant flow rate and cooling modes on the thermal behaviour of the battery module through numerical simulations and experiments. As a result, they found that increasing the coolant flow rate reduces the maximum temperature and provides homogeneous temperature distribution [24].

In this study, two factors affecting the cooling performance of lithium-ion batteries were selected and investigated using numerical methods. These were determined using air flow geometry design and different Reynolds numbers. First, the differences between a classical flow path design (Z channel), where the air inlets and outlets are in the same direction, and an alternative design (U channel), where the air inlets and outlets are in different directions, were evaluated. To understand the effect of the turbulent properties of the fluid in both designs, the analyses performed using different Reynolds numbers (Re=4000, 6000, 8000, 10000, 15000) were compared with each other.

## 2. MATERİAL AND METHODS

### 2.1. Design

In lithium-ion battery systems, flow zones are created between the cells in the internal structure to provide airflow. These openings play an essential role in cooling the batteries through heat transfer. In such systems, air channels between the cells allow the heat to be effectively distributed and removed. The design of the air channels between the cells significantly affects the efficiency of the battery cooling system. Geometric features such as channel width, height and length significantly affect the air flow rate and pressure drop. For example, comprehensive and low-resistance channels provide higher airflow and allow for more effective cooling performance. On the other hand, narrow and long channels can cause higher pressure drops and limit airflow.

Another critical point in lithium-ion battery designs is the design changes in the air inlet and outlet regions. Differences in the inlet and outlet designs between cells significantly affect the flow regime and heat transfer efficiency. The design of the inlet region determines the flow of the inlet and its distribution inside the cell. An irregular air distribution leads to a heterogeneous flow regime, causing turbulence formation and improvement in heat transfer. The design of the outlet region affects the movement of the flow between the cells. Inadequate outlet design can reduce heat transfer efficiency by causing pressure increase and, thus, flow rate decrease. Therefore, optimizing the inlet and outlet regions to provide homogeneous and high-speed airflow in the internal channels can maximize heat transfer between cells. The symmetrical inlet-outlet design allows the formation of turbulent flow regimes and effective heat removal.

This study modelled lithium-ion battery cells with two different inlet and outlet designs using a CAD program in a three-dimensional environment. The difference between the designs is the air inlet and outlet directions in one of them. The design shown in Figure 1 is a Z-channel lithium-ion battery. In this geometry, the inlet and outlet directions of the cooling air are the same. The design shown in Figure 2 is a U-channel lithium-ion battery. In this geometry, the inlet and outlet directions of the cooling air are different. The dimensions of the batteries used in this study are also given in Figures 1 and 2. In addition, the dimensions and locations of the nickel-based cathode materials in the battery's internal structure are also shown in Figure 3.

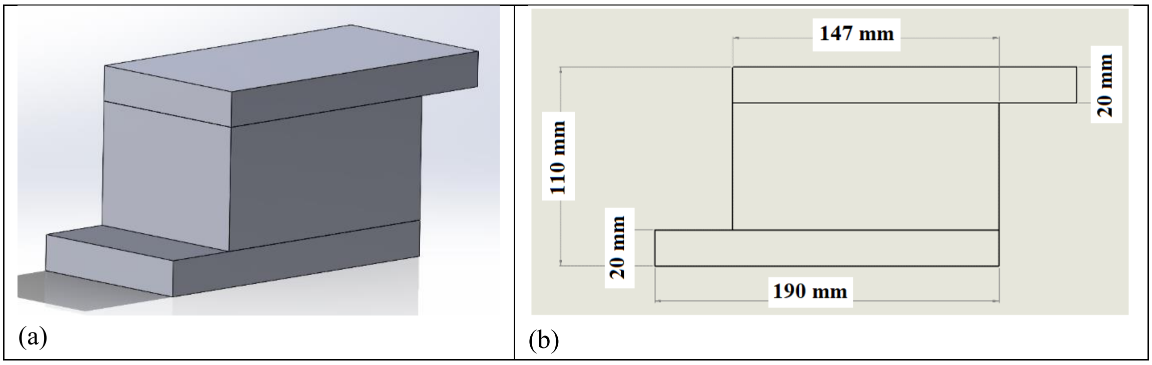


**Figure 1. Z channel (a) General view, (b) Dimensioned version**

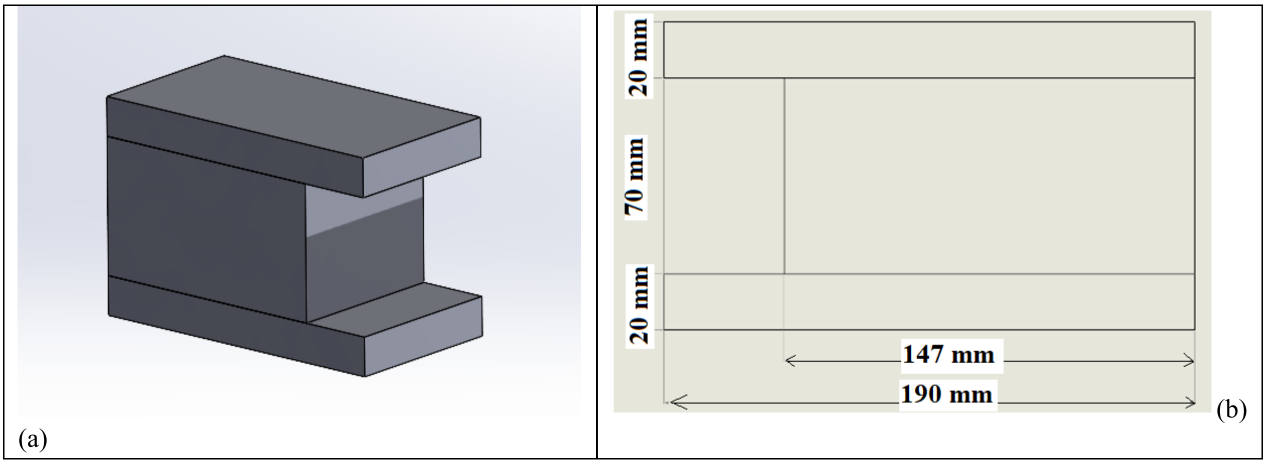


**Figure 2. U channel (a) General view, (b) Dimensioned version**

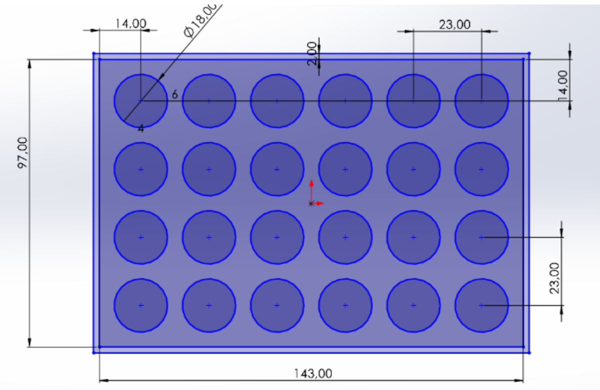


**Figure 3. The positions of nickel-based cathode materials within the battery**

### 2.2. Mesh Process

The mesh structure used for finite element analysis (FEA) is an essential factor that determines the accuracy and precision of the analysis. A quality mesh structure ensures the finite element analysis results are more accurate and reliable. In the analyses performed in this study, mesh structures consisting of approximately 4 million cells composed of square elements were used. The general appearance of the mesh structures created for the Z and U channels is given in Figure 4

.

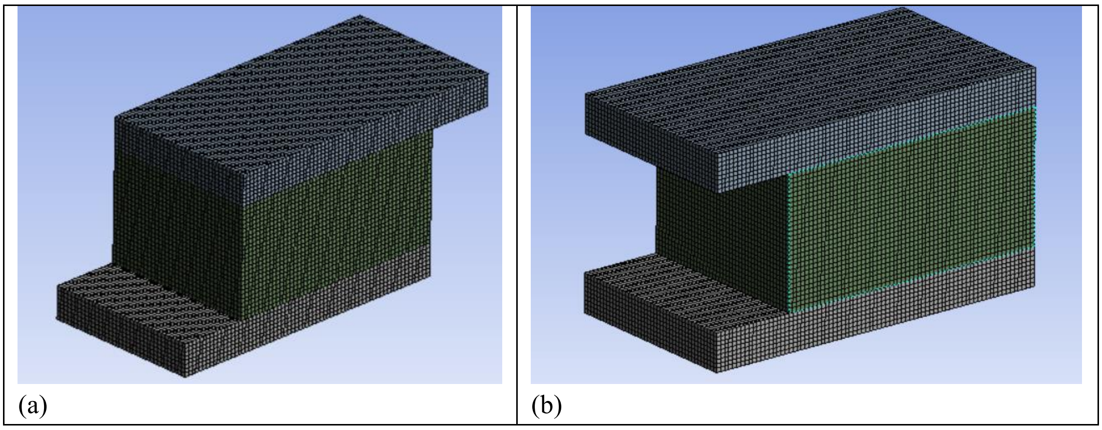


**Figure 4. The general appearance of mesh structure (a) Z-channel, (b) U-channel**

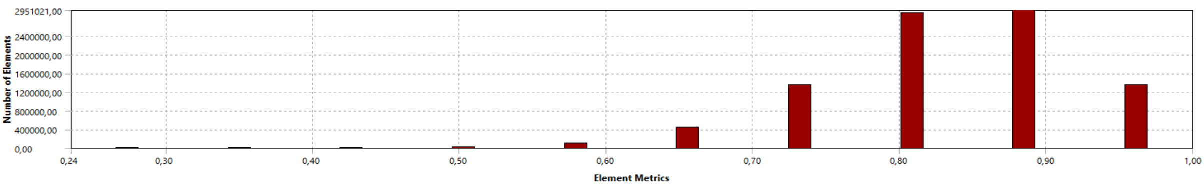


**Figure 5. Element quality values**

Element quality is a criterion that controls an element's geometric order and numerical balance. The quality of an element varies depending on factors such as the element's size, shape and location. The high element quality in the created mesh order allows the mesh structure to provide more accurate results. The element quality value is a parameter based on the geometric properties of the element, such as edge lengths, angles and corner joint angles. Element quality is generally a number between 0 and 1. An element quality close to 1 provides better results. In the mesh network structure created for analysing the lithium-ion battery cooling system, more than 90% of the materials are between 0.9 and 1. The element quality values are shown in detail in Figure 5. Therefore, the element qualities of the mesh network structure are suitable for analysis accuracy

.

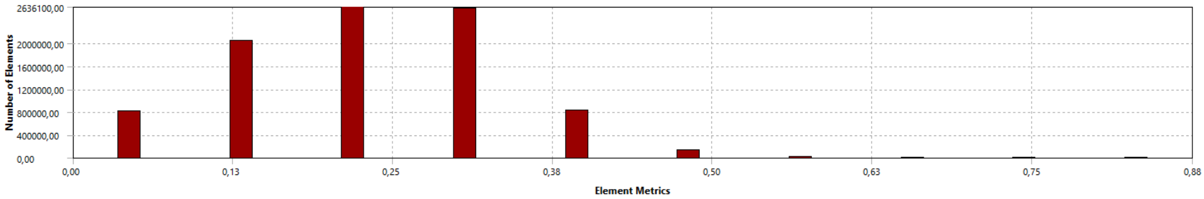


**Figure 6. Skewness values**

Skewness is a measure of the curvature of the elements in the mesh structure used for finite element analysis. The high curvature values in the mesh structure mean that the components can be subjected to high levels of deformation at the same rate. This can affect the accuracy and reliability of the finite element analysis results. The skewness measure considers the angles between the element's edges and the angular difference of the most giant angled triangle of the component. Skewness is generally a number between 0 and 1. A skewness close to 0 provides better results. The skewness values of the mesh network structure created for the Lithium-ion Battery cooling system analysis in the study are an average of 0.25. The skewness quality values are shown in detail in Figure 6. This average value indicates that the mesh network structure is suitable for analysis after skewness examination.

### 2.3. Material

Lithium cobalt oxide ($LiCoO_2$) compound is a vital cathode material in lithium-ion batteries. $LiCoO_2$ has a stable chemical structure, which ensures long battery life and safe operation. $LiCoO_2$ is also one of lithium-ion batteries' oldest and most widely used cathode materials. Considering these advantages, $LiCoO_2$ is an important cathode material in lithium-ion battery technology. Table 1 shows the thermophysical properties of $LiCoO_2$ material [25].

**Table 1. Thermophysical properties of lithium cobalt oxide ($LiCoO_2$)**

| | |
|---|---|
| Density (ρ) | 5000 (kg/m$^3$) |
| Thermal Conductivity (λ) | 10 (W/m.K) |
| Specific Heat Capacity ($c_p$) | 800 (J/kg·K) |
| Thermal Expansion Coefficient (α) | $1.5 \times 10^{-5}$ (1/K) |
| Emissivity (ε) | 0.3 |
| Melting Point | 1273 (K) |

### 2.4. CFD Modelling

CFD (Computational Fluid Dynamics) programs are used to model the behaviour of fluids using computer-based numerical analysis methods. These analyzes provide data to the user by solving relevant mathematical equations to estimate fluids' speed, pressure, temperature, density and other properties [26]. CFD analysis is a widely used tool in solving engineering problems. CFD programs are frequently used in industrial fields, especially automotive and aviation [27]. The CFD method is increasingly used every day because it allows you to save both time and money. One of the most significant advantages of CFD analysis is that it can be used at any stage, eliminating the need for a physical prototype. Numerical analysis has also replaced the old applications of experimental testing on lithium-ion battery components. With the analysis performed for lithium-ion batteries, it is possible to optimize the performance of battery packs and predict overheating. Numerical methods can also be used to optimize the design of battery packs and to determine the airflow required for cooling the packs. In short, CFD analysis plays a vital role in developing lithium-ion battery technology. In this way, improving and optimising battery designs cost-effectively and efficiently is possible [28].

In this study, SST k-ω is used as the turbulence model. SST k-ω is one of the most frequently used models for calculating turbulence in near-wall and free-flow regions. SST k-ω model uses the classical k-ω model in near-wall regions while switching to the k-epsilon model in free-flow regions. The

SST k-ω model is based on two equations. These are k and ω. k represents the energy of turbulence. ω represents the frequency of turbulence. SST (Shear Stress Transport) combines the advantages of these two models and is widely preferred, especially in aerodynamics and flow separation calculations. This model was developed to increase the accuracy in turbulent flows [29].

In the analyses, two different battery temperatures were used. These were selected as 40 ºC and 60 ºC. In all calculations made for Re=4000, 6000, 8000, 10000, and 15000, air at 20 ºC was used as the coolant. The boundary conditions used for designs with different air flow directions are given in Figure 7. Steady-state analyses were conducted over 20,000 steps. The computer used in this study was equipped with an Intel Core i7 processor with 16 cores and 64 GB of RAM. Each analysis required approximately 6 hours to complete.

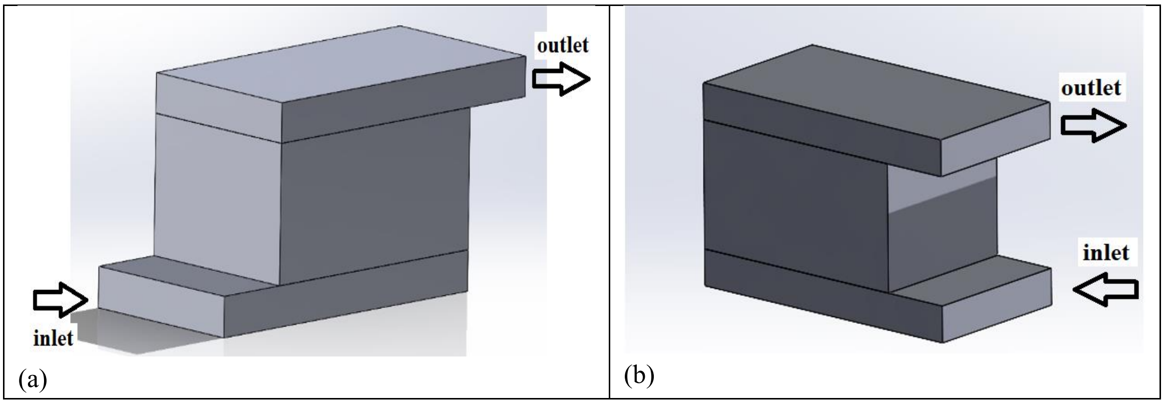


**Figure 7. Boundary conditions of li-ion battery (a) Z-channel, (b) U-channel**

This study calculated the Nu number to evaluate the heat transfer efficiency of two packages designed for lithium-ion batteries with different air inlet and outlet directions. The estimated values were compared with each other. In this study, the flow was assumed to be turbulent at all Reynolds numbers used. Therefore, it was believed that the flow was turbulent along the channel. However, since it is known that turbulent flow is generally concentrated in regions where vortices are formed, it was predicted that the turbulence effect would be more significant in some areas. Therefore, the values used in calculating the Nusselt number were taken from the regions where nickel-based cathode materials are located in the inner area of the battery at the end of the numerical analysis. The calculation of the Nusselt number (Nu) is given in Equation 1.

$$Nu = \frac{h.D_h}{k} \quad (1)$$

k and h represent thermal conductivity and heat transfer coefficient, respectively [30].

## 3. RESULTS

### 3.1. Thermal Analysis Results for the Z-Channel Design of a Battery at 60 °C

The Z-channel lithium-ion battery design, modelled three-dimensionally according to the specified technical dimensions using the CAM program, was subjected to flow analyses using the CFD program under a cell temperature of 60°C, with variable speed data based on five different Reynolds numbers. Figures 8, 9, and 10 show the resulting temperature distributions from these analyses

.

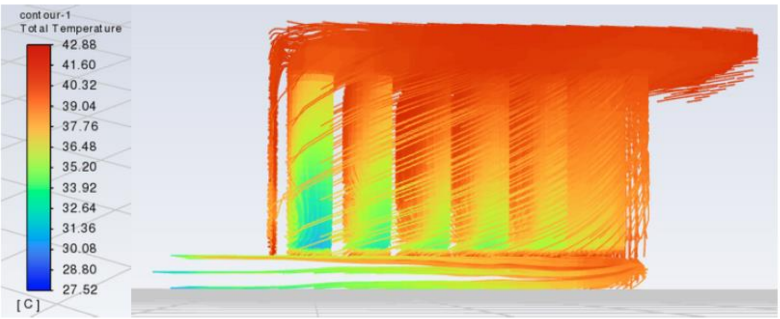


**Figure 8. Contour of the Temperature Distribution for the Z-Channel Battery at Re = 4000 under 60 °C Operational Temperature**

The velocity for analysing the Z channel type lithium-ion battery at the Re=4000 boundary condition at 60° operating temperature was calculated as 0.414 m/s. The maximum temperature value was measured as 42.88 °C, as can be seen in Figure 8, due to the analysis performed according to the entered boundary conditions.

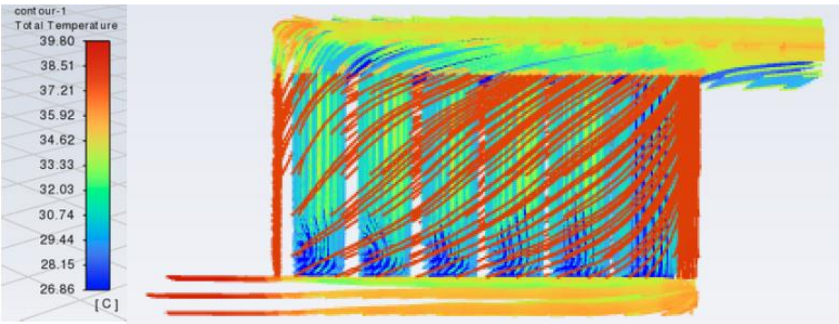


**Figure 9. Contour of the Temperature Distribution for the Z-Channel Battery at Re = 8000 under 60 °C Operational Temperature**

The velocity for analysing the Z channel type lithium-ion battery at the Re=8000 boundary condition at 60° operating temperature was calculated as 0.828 m/s. The maximum temperature value was measured as 39.80 °C, as can be seen in Figure 9, due to the analysis performed according to the entered boundary conditions.

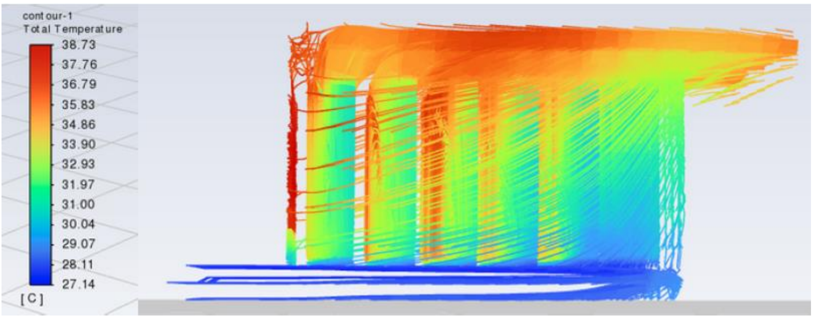


**Figure 10. Contour of the Temperature Distribution for the Z-Channel Battery at Re = 15000 under 60 °C Operational Temperature**

The velocity for analysing the Z channel type lithium-ion battery at the Re=15000 boundary condition at 60° operating temperature was calculated as 1.552 m/s. The maximum temperature value was measured as 38.73 °C, as can be seen in Figure 10, due to the analysis performed according to the entered boundary conditions.

### 3.2. Thermal Analysis Results for the U-Channel Design of a Battery at 60°C

The U-channel lithium-ion battery design, modelled three-dimensionally according to the specified technical dimensions using the CAM program, was subjected to flow analyses using the CFD program under a cell temperature of 60°C, with variable speed data based on five different Reynolds numbers. Figures 11, 12, and 13 show the resulting temperature distributions from these analyses.

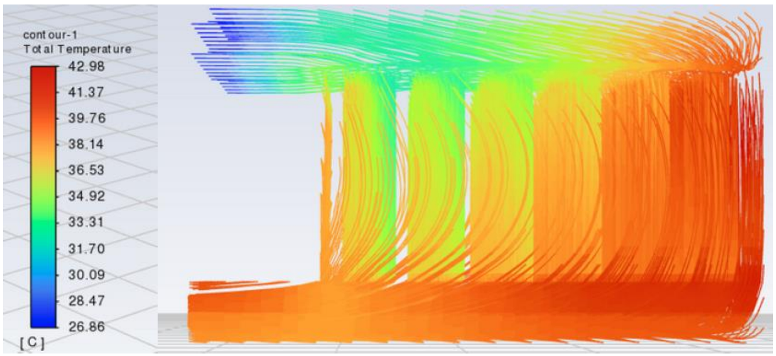


**Figure 11. Contour of the Temperature Distribution for the U-Channel Battery at Re = 4000 under 60 °C Operational Temperature**

The velocity for analysing the U channel type lithium-ion battery at the Re=4000 boundary condition at 60° operating temperature was calculated as 0.414 m/s. The maximum temperature value was measured as 42.98 °C, as can be seen in Figure 11, due to the analysis performed according to the entered boundary conditions.

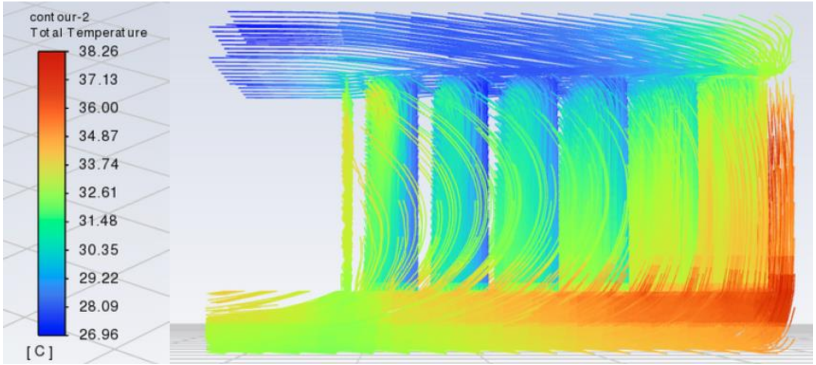


**Figure 12. Contour of the Temperature Distribution for the U-Channel Battery at Re = 8000 under 60 °C Operational Temperature**

The velocity for analysing the U channel type lithium-ion battery at the Re=8000 boundary condition at 60° operating temperature was calculated as 0.828 m/s. The maximum temperature value was measured as 38.26 °C, as can be seen in Figure 12, due to the analysis performed according to the entered boundary conditions.

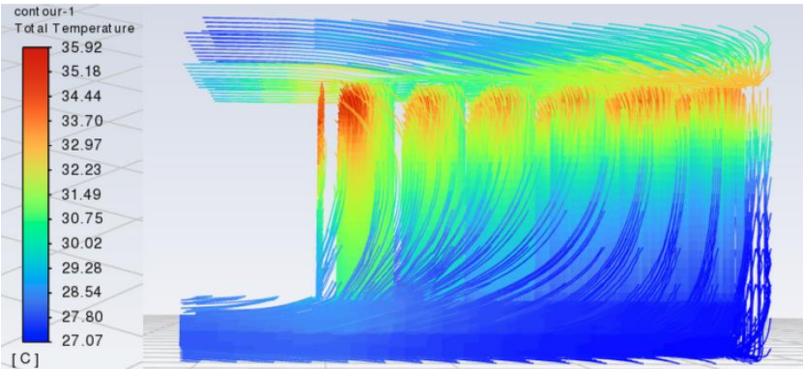


**Figure 13. Contour of the Temperature Distribution for the U-Channel Battery at Re = 15000 under 60 °C Operational Temperature**

The velocity for analysing the U channel type lithium-ion battery at the Re=15000 boundary condition at 60° operating temperature was calculated as 1.525 m/s. The maximum temperature value was measured as 35.92 °C, as can be seen in Figure 13, due to the analysis performed according to the entered boundary conditions.

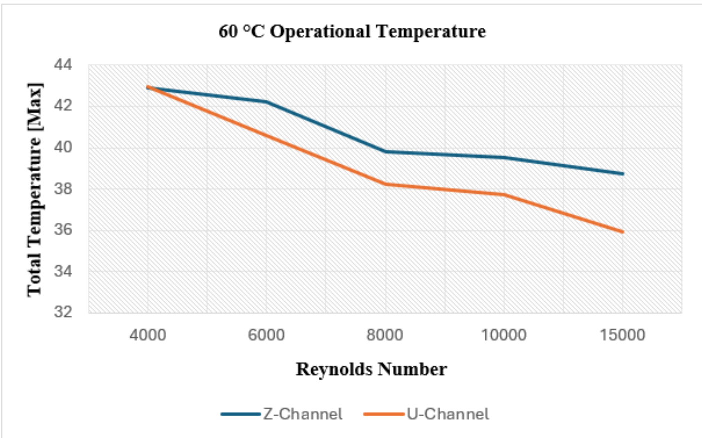


**Figure 14. Comparison of Maximum Temperature Values for Z-Channel and U-Channel Designs at 60°C Operational Temperature Across Various Reynolds Numbers**

Figure 14 compares maximum temperature values obtained from all analyses performed for both Z-channel and U-channel designs under different Reynolds numbers at the 60 °C temperature of a lithium-ion battery. This graph highlights the thermal performance trade-offs between Z-channel and U-channel designs by clearly visualising how the temperature distribution responds to different flow conditions for each channel type. These results are crucial for understanding the thermal management efficiency in lithium-ion batteries under increased turbulent flow.

### 3.3. Thermal Analysis Results for the Z-Channel Design of a Battery at 40°C

The Z-channel lithium-ion battery design, modelled three-dimensionally according to the specified technical dimensions using the CAM program, was subjected to flow analyses using the CFD program under a cell temperature of 40°C, with variable speed data based on five different Reynolds numbers. Figures 15, 16, and 17 show the resulting temperature distributions from these analyses.

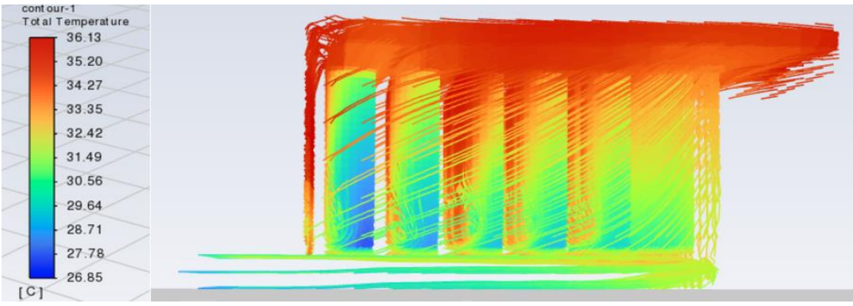


**Figure 15. Contour of the Temperature Distribution for the Z-Channel Battery at Re = 4000 under 40 °C Operational Temperature**

The velocity for analysing the Z channel type lithium-ion battery at the Re=4000 boundary condition at 40° operating temperature was calculated as 0.414 m/s. The maximum temperature value was measured as 36.13 °C, as can be seen in Figure 15, due to the analysis performed according to the entered boundary conditions.

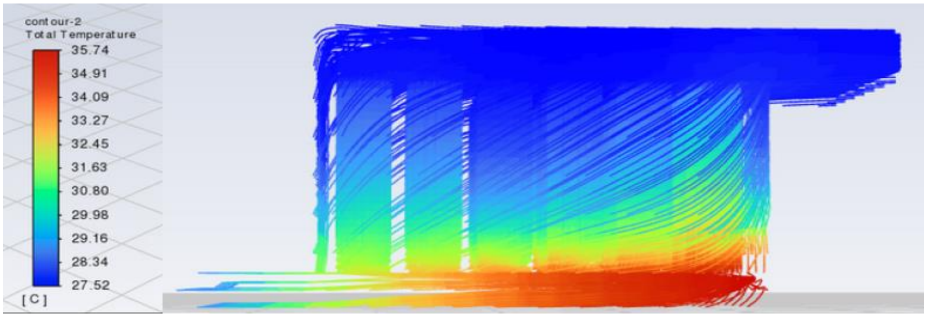


**Figure 16. Contour of the Temperature Distribution for the Z-Channel Battery at Re = 8000 under 40 °C Operational Temperature**

The velocity for analysing the Z channel type lithium-ion battery at the Re=8000 boundary condition at 40° operating temperature was calculated as 0.828 m/s. The maximum temperature value was measured as 35.74 °C, as can be seen in Figure 16, due to the analysis performed according to the entered boundary conditions.

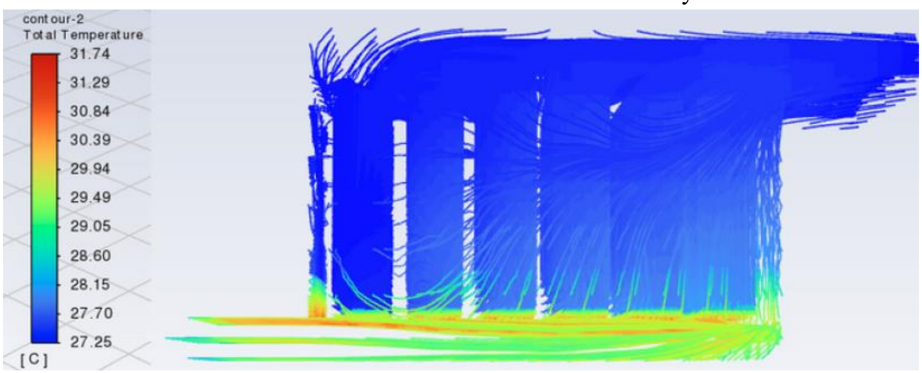


**Figure 17. Contour of the Temperature Distribution for the Z-Channel Battery at Re = 15000 under 40 °C Operational Temperature**

The velocity for analysing the Z channel type lithium-ion battery at the Re=15000 boundary condition at 40° operating temperature was calculated as 1.525 m/s. The maximum temperature value was measured as 31.74 °C, as can be seen in Figure 17, due to the analysis performed according to the entered boundary conditions.

### 3.4. Thermal Analysis Results for the U-Channel Design of a Battery at 40°C

The U-channel lithium-ion battery design, modelled three-dimensionally according to the specified technical dimensions using the CAM program, was subjected to flow analyses using the CFD program under a cell temperature of 40°C, with variable speed data based on five different Reynolds numbers. Figures 18, 19, and 20 show the resulting temperature distributions from these analyses.

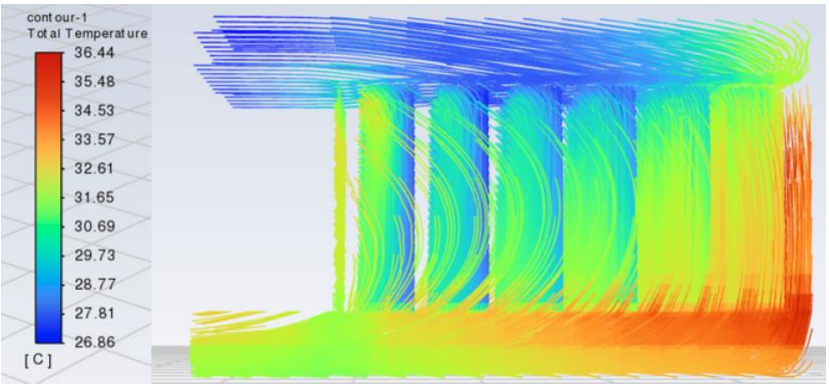


**Figure 18. Contour of the Temperature Distribution for the U-Channel Battery at Re = 4000 under 40 °C Operational Temperature**

The velocity for analysing the U channel type lithium-ion battery at the Re=4000 boundary condition at 40° operating temperature was calculated as 0.414 m/s. The maximum temperature value was measured as 36.44 °C, as can be seen in Figure 18, due to the analysis performed according to the entered boundary conditions

.

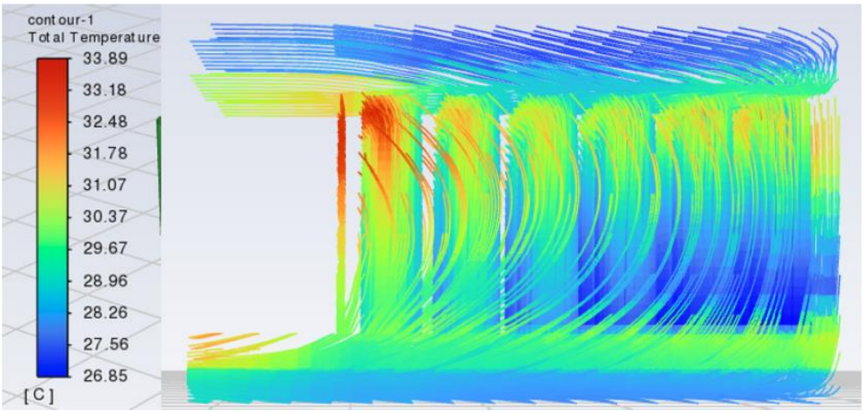


**Figure 19. Contour of the Temperature Distribution for the U-Channel Battery at Re = 8000 under 40 °C Operational Temperature**

The velocity for analysing the U channel type lithium-ion battery at the Re=8000 boundary condition at 40° operating temperature was calculated as 0.828 m/s. The maximum temperature value was measured as 33.89 °C, as can be seen in Figure 19, due to the analysis performed according to the entered boundary conditions.

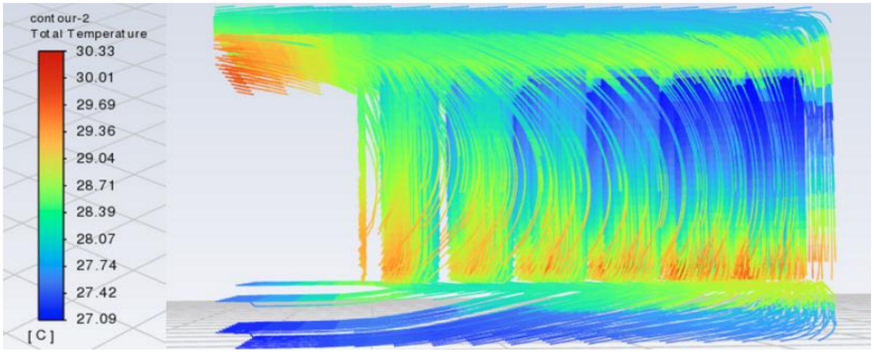


**Figure 20. Contour of the Temperature Distribution for the U-Channel Battery at Re = 15000 under 40 °C Operational Temperature**

The velocity for analysing the U channel type lithium-ion battery at the Re=15000 boundary condition at 40° operating temperature was calculated as 1.525 m/s. The maximum temperature value was measured as 30.33 °C, as can be seen in Figure 20, due to the analysis performed according to the entered boundary conditions.

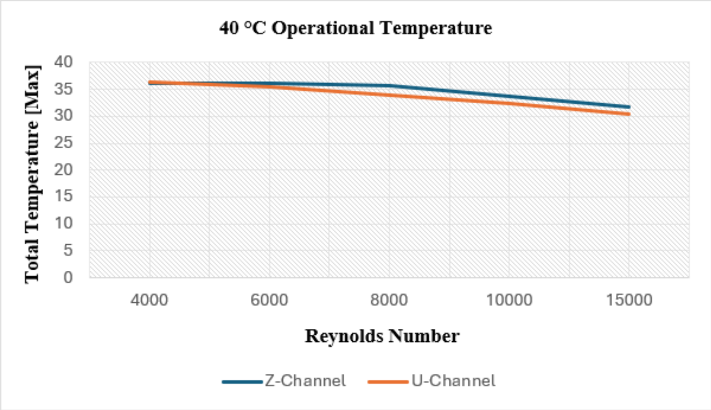


**Figure 21. Comparison of Maximum Temperature Values for Z-Channel and U-Channel Designs at 40°C Operational Temperature Across Various Reynolds Numbers**

Figure 21 compares maximum temperature values obtained from all analyses performed for Z-channel and U-channel designs under different Reynolds numbers at the 40 °C temperature of a lithium-ion battery. This graph highlights the thermal performance trade-offs between Z-channel and U-channel designs by clearly visualising how the temperature distribution responds to different flow conditions for each channel type. These results are crucial for understanding the thermal management efficiency in lithium-ion batteries under increased turbulent flow

.

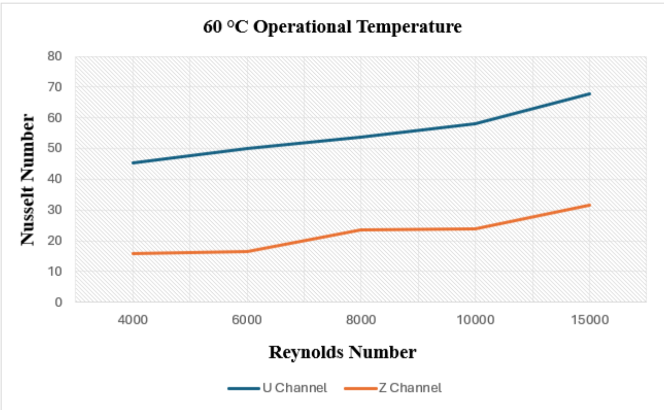


**Figure 22. Comparison of Nusselt Numbers for Z-Channel and U-Channel Designs at 60°C Operational Temperature Across Various Reynolds Numbers**

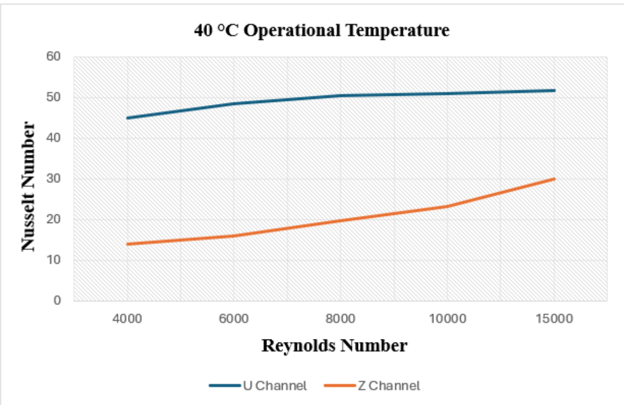


**Figure 23. Comparison of Nusselt Numbers for Z-Channel and U-Channel Designs at 40 °C Operational Temperature Across Various Reynolds Numbers**

Figures 22 and 23 compare Nusselt numbers for U-channel and Z-channel lithium-ion battery designs under operational temperatures of 40 °C and 60 °C. The analysis reveals that the Nusselt number is consistently higher in the U-channel design. As the Reynolds number increases, the turbulence within the flow intensifies, leading to a corresponding increase in Nusselt values. These findings indicate that the heat transfer efficiency of the U-channel design is better than the Z-channel design, especially under higher turbulent flow conditions.

**4. CONCLUSİONS**

In this study, numerical analyses were performed using different parameters to predict the thermal management of lithium-ion batteries. As a result of numerical calculations made for increasing Reynolds numbers using two different battery operating temperatures, the effect of airflow direction was investigated. The obtained results showed that the opposite airflow direction battery design called the U-type channel, is more advantageous in cooling the nickel strips and homogeneous temperature distribution than the same airflow direction design called the Z-type channel. In addition, it was observed that Nu numbers increase with the Reynolds number. Based on these results, it is recommended that a U-type channel design be used as it provides more effective cooling for lithium-ion batteries operating at high speeds and exposed to high operating temperatures to operate at optimum temperatures. In the continuation of this study, the most efficient cooling strategy can be determined by changing the channel width, depth and position of nickel strips to optimize the U-type channel design.

**REFERENCES**

1. Nasajpour-Esfahani, N., Garmestani, H., Bagheritabar, M., Jasim, D., Toghraie, D., Dadkhah, S., & Firoozeh, H. (2024). Comprehensive review of lithium-ion battery materials and development challenges. Renewable and Sustainable Energy Reviews, 203, 114783.
2. An, Z., Zhang, J., Gao, W., Liu, H., & Gao, Z. (2024). Lightweight hybrid lithium-ion battery thermal management system based on 3D-printed scaffold. Journal of Energy Storage, 78, 110141.
3. Yamashita, A., Berg, S., & Figgemeier, E. (2024). Unsupervised learning of charge-discharge cycles from various lithium-ion battery cells to visualize dataset characteristics and to interpret model performance. Energy and AI, 17, 100409.
4. Shi, H., Luo, Y., Yin, C., & Ou, L. (2024). Review of the application of ionic liquid systems in achieving green and sustainable recycling of spent lithium-ion batteries. Green Chemistry, 26(14), 8100-8122.
5. Chauhan, R., Santran, R., Obrecht, M., & Singh, R. (2024). Energy storage potential of used electric vehicle batteries for supporting renewable energy generation in India. Energy for Sustainable Development, 81, 101513.
6. Hu, C., Ye, H., Jain, G., & Schmidt, C. (2018). Remaining useful life assessment of lithium-ion batteries in implantable medical devices. Journal of Power Sources, 375, 118-130.
7. Xu, X., Han, X., Lu, L., Wang, F., Yang, M., Liu, X., Wu, Y., Tang, S., Hou, Y., Hou, J., Yu, C., & Ouyang, M. (2024). Challenges and opportunities toward long-life lithium-ion batteries. Journal of Power Sources, 603, 234445.
8. Akbarzadeh, M., Kalogiannis, T., Jaguemont, J., Jin, L., Behi, H., Karimi, D., Beheshti, H., Mierlo, J., & Berecibar, M. (2021). A comparative study between air cooling and liquid cooling thermal management systems for a high-energy lithium-ion battery module. Applied Thermal Engineering, 198, 117503.
9. Chen, D., Jiang, J., Kim, G., Yang, C., & Pesaran, A. (2016). Comparison of different cooling methods for lithium-ion battery cells. Applied Thermal Engineering, 94, 846-854.
10. Sen, M., Ozcan, M., & Eker, Y. (2024). A review on the lithium-ion battery problems used in electric vehicles. Next Sustainability, 3, 100036.
11. Deng, Y., Feng, C., Jiaqiang, E., Zhu, H., Chen, J., Wen, M., & Yin, H. (2018). Effects of different coolants and cooling strategies on the cooling performance of the power lithium ion battery system: A review. Applied Thermal Engineering, 142, 10–29.
12. Thakur, A., Prabakaran, R., Elkadeem, M., Sharshir, S., Arıcı, M., Wang, C., Zhao, W., Hwang, J., & Saidur, R. (2020). A state of the art review and future viewpoint on advance cooling techniques for Lithium-ion battery system of electric vehicles. Journal of Energy Storage, 32, 101771.
13. Sun, H., & Dixon, R. (2014). Development of cooling strategy for an air-cooled lithium-ion battery pack. Journal of Power Sources, 272, 404-414.
14. Xun, J., Liu, R., & Jiao, K. (2013). Numerical and analytical modeling of lithium ion battery thermal behaviors with different cooling designs. Journal of Power Sources, 233, 47-61.
15. Saw, L., Ye, Y., Tay, A., Chong, W., Kuan, S., & Yew, M. (2016). Computational fluid dynamic and thermal analysis of Lithium-ion battery pack with air cooling. Applied Energy, 177, 783–792.
16. Shang, Z., Qi, H., Liu, X., Ouyang, C., & Wang, Y. (2019). Structural optimization of lithium-ion

battery for improving thermal performance based on a liquid cooling system. International Journal of Heat and Mass Transfer, 130, 33–41.

17. Chavan, S., Venkateswarlu, B., Prabakaran, R., Salman, M., Joo, S., Choi, G., & Kim, S. (2023). Thermal runaway and mitigation strategies for electric vehicle lithium-ion batteries using battery cooling approach: A review of the current status and challenges. Journal of Energy Storage, 72, 108569.
18. Wang, T., Tseng, K., & Zhao, J. (2015). Development of efficient air-cooling strategies for lithium-ion battery module based on empirical heat source model. Applied Thermal Engineering, 90, 521-529.
19. Park, H. (2013). A design of air flow configuration for cooling lithium ion battery in hybrid electric vehicles. Journal of Power Sources, 239, 30-36.
20. Yang, T., Yang, N., Zhang, X., & Li, G. (2016). Investigation of the thermal performance of axial-flow air cooling for the lithium-ion battery pack. International Journal of Thermal Sciences, 108, 132-144.
21. Kizilel, R., Sabbaha, R., Selman, J., & Al-Hallaj, S. (2009). An alternative cooling system to enhance the safety of Li-ion battery packs. Journal of Power Sources, 194, 1105–1112.
22. Wang, T., Tseng, K., Zhao, J., & Wei, Z. (2014). Thermal investigation of lithium-ion battery module with different cell arrangement structures and forced air-cooling strategies. Applied Energy, 134, 229–238.
23. Kirad, K., & Chaudhari, M. (2021). Design of cell spacing in lithium-ion battery module for improvement in cooling performance of the battery thermal management system. Journal of Power Sources, 481, 229016.
24. Wang, H., Tao, T., Xu, J., Mei, X., Liu, X., & Gou, P. (2020). Cooling capacity of a novel modular liquid-cooled battery thermal management system for cylindrical lithium ion batteries. Applied Thermal Engineering, 178, 115591.
25. Wanga, G., Bia, Z., Zhanga, A., Dasa, P., Lina, H., & Wu, Z. (2024). High-Voltage and Fast-Charging Lithium Cobalt Oxide Cathodes: From Key Challenges and Strategies to Future Perspectives. Engineering, 37, 105–127.
26. Moraga, N., & Rivera, D. (2021). Advantages in predicting conjugate freezing of meat in a domestic freezer by CFD with turbulence k- ε 3D model and a local exergy destruction analysis. International Journal of Refrigeration, 126, 76–87.
27. Kumar, M., Muniyappan, M., & Selvan, S. (2024). Experimental and CFD analysis on the impact of hydrogen as fuel on the behavior of a passenger car gasoline direct injection engine. Journal of the Energy Institute, 113, 101487.
28. Hasan, H., Togun, H., Mohammed, H., Abed, A., & Homod, R. (2023). CFD simulation of effect spacing between lithium-ion batteries by using flow air inside the cooling pack. Journal of Energy Storage, 72, 108631.
29. Younoussi, S., & Ettaouil, A. (2024). Calibration method of the k-ω SST turbulence model for wind turbine performance prediction near stall condition. Journal of Energy Institute, 10(1), 24048.
30. Zhao, H., Li, X., & Wu, X. (2018). New friction factor and Nusselt number equations for turbulent convection of liquids with variable properties in circular tubes. International Journal of Heat and Mass Transfer, 124, 454-462.